

r, Phe, Lys, Trpn, Dap)を標準に用いる測定方法により(Kanno J, et al., BMC Genomics, 2006)、細胞当たりmRNAコピー数を測定した。その結果、1) Indigo, indirubinがCYP1A1 mRNAコピー数を60倍以上増加させるのに対し、DIMの効果は3倍程度であること、2)細胞内ER- α とAhR mRNAのコピー数の比は約2:1とほぼ同水準であり、相互作用による蛋白分解制御が起こる上で妥当な量比であること、が明らかとなった。各用量におけるER蛋白分解活性と遺伝子発現誘導活性をプロットしたところ、DIMにおいて両者機能の明確な乖離が観察された。

(4) DIMのER蛋白分解促進能に関するAhR依存性の検討

DIMによるER蛋白分解促進機能がAhRを介していることを確認するため、MCF7細胞においてAhRをノックダウンした。その結果、DIMによるER蛋白分解の促進はAhR依存的事であることが示された。また、ユビキチン鎖イニシエーションに関わるE2酵素であるUBCH5ファミリーをノックダウンした結果、DIM依存的なAhRの蛋白分解が抑制されていた。この結果から、DIMの効果はユビキチン・プロテアソーム系を介した蛋白分解制御であることが示唆された。

D. 考察

エストロゲン受容体(ER)は乳癌克服に向けて重要な分子標的であり、本研究では新たなER機能阻害戦略の分子基盤構築のため、ER蛋白分解機構の解析に取り組んだ。AhR活性化によるER蛋白分解の促進の分

子機構を解析する上で、本年度は特に特異的リガンドの探索と解析を行った。その結果、AhRの転写促進機能を微弱にしか活性化しない部分アンタゴニストの一つが、ER蛋白分解活性の強力なアゴニストとして機能することを見出した。本年度の結果から、AhRによる転写機能と蛋白分解促進能は独立した分子機能であると考えられた。すなわち、AhRの蛋白分解促進能のみを選択的に活性化させることによるER機能阻害戦略の有効性を示唆するものである。

AhRによる転写活性や蛋白分解活性は、細胞培養条件などによる細胞周期やシグナル伝達経路によって変化する可能性が考えられる。本研究では、両活性が少なくとも一つの条件下で乖離することを見出したが、より生理的条件やin vivoでの影響評価については今後検討が必要と考えられる。

また、蛋白分解に選択性を有する低分子リガンドは、ER蛋白分解機構を解析する上での有効なモデル系になるものと期待される。そこで今後はこの系をモデル系として、さらなる分解促進因子や関連因子の同定や、分子機構解析を進める。また、転写制御活性と乖離したER機能阻害を有する低分子リガンドの探索系を構築する上で、今回同定したリガンドを陽性対照として系の構築に応用が期待される。

E. 結論

本分担研究ではエストロゲン受容体の蛋白分解機構を解析した。AhRによるER蛋白分解を選択的に促進する因子の一つとして、3,3'-diindolylmethane (DIM)を見出した。DIMはAhR部分アンタゴニストとして報告されているが、定量的な比較検討の結果、E

R蛋白分解活性においては選択的なアゴニストとして機能し、ER蛋白分解を促進することを見出した。DIMを用いた解析の結果、AhR依存的なER蛋白分解促進が転写活性とは独立した分子機構であることが示唆された。本結果はER蛋白分解の分子機構解明の重要な手がかりとなると考えられる。

G. 研究発表

1. 論文発表

なし

2. 学会発表

なし

H. 知的財産権の出願・登録状況

(予定を含む。)

1. 特許取得

なし

2. 実用新案登録

なし

3.その他

なし

研究成果の刊行に関する一覧表

書籍

著者氏名	論文タイトル名	書籍全体の編集者名	書籍名	出版社名	出版地	出版年	ページ
該当なし							

雑誌

発表者氏名	論文タイトル名	発表誌名	巻号	ページ	出版年
Kawazu, M., Ueno, T., Kontani, K., Ogita, Y., Ando, M., Fukumura, K., Yamato, A., Soda, M., Takeuchi, K., Miki, Y., Yamaguchi, H., Yasuda, T., Naoe, T., Yamashita, Y., Katada, T., Choi, Y.L. and Mano, H.	Transforming mutations of RAC guanosine triphosphatases in human cancers.	Proc Natl Acad Sci USA.	110	3029-34	2013
Iyevleva, A.G., Kuligina, E., Mitiushkina, N.V., Togo, A.V., Miki, Y. and Imyanitov, E.N.	High level of miR-21, miR-10b, and miR-31 expression in bilateral vs. unilateral breast carcinomas.	Breast Cancer Res Treat,	131	1049-59	2012
Komatsu M, Yoshimaru T, Matsuo T, Kiyotani K, Miyoshi Y, Tanahashi T, Rokutan K, Yamaguchi R, Saito A, Miyano S, Nakamura Y, Sasa M, Shimada M, Katagiri T.	Molecular features of triple negative breast cancers by genome-wide gene expression profiling analysis.	Int J Oncol.	42	478-506	2013

Elgazzar S, Zembutsu H, Takahashi A, Kubo M, Aki F, Hirata K, Takatsuka Y, Okazaki M, Ohsumi S, Yamakawa T, Sasa M, Katagiri T, Miki Y, Nakamura Y.	A genome-wide association study identifies a genetic variant in the SIAH2 locus associated with hormonal receptor- positive breast cancer in Japanese.	J Hum Genet. 56		766-771.	2012
Murase K, Yanai A, Saito M, Imamura M, Miyagawa Y, Takatsuka Y, Inoue N, Ito T, Hirota S, Sasa M, Katagiri T, Fujimoto Y, Hatada T, Ichii S, Nishizaki T, Tomita N, Miyoshi Y.	Biological characteristics of luminal subtypes in pre- and postmenopausal estrogen receptor-positive and HER2-negative breast cancers.	Breast Cancer.	In press		2013
Sato K, Sundaramoorthy E, Rajendra E, Hattori H, Jeyasekharan AD, Ayoub N, Schiess R, Aebersold R, Nishikawa H, Sedukhina AS, Wada H, Ohta T, Venkitaraman AR.	A DNA-Damage Selective Role for BRCA1 E3 Ligase in Claspin Ubiquitylation, CHK1 Activation, and DNA Repair.	Curr Biol.	22 (18)	1659-66	2012
Shinichiro Nakada, Rikako Miyamoto Yonamine, Koichi Matsuo	RNF8 regulates assembly of RAD51 at DNA double-strand breaks in the absence of BRCA1 and 53BP1.	Cancer Research	72	4974-83.	2012
Tokuda, E., Seino, Y., Arakawa, A., Saito, M., Kasumi, F., Hayashi, S., and Yamaguchi, Y.	Estrogen receptor- α directly regulates sensitivity to paclitaxel in neoadjuvant chemotherapy for breast cancer.	Breast Cancer Res. Treat.	133(2)	427-36	2012
Kataoka, M., Yamaguchi, Y., Moriya, Y., Sawada, N., Yasuno, H., Kondoh, K., Evans, DB., Mori, K., and Hayashi, S.	Antitumor activity of chemo-endocrine therapy in premenopausal and postmenopausal models with human breast cancer xenografts.	Oncology Reports	27	303-310	2012

Takagi, K., Moriya, T., Kurosumi, M., Oka, K., Miki, Y., Ebata, A., Toshima, T., Tsunekawa, S., Takei, H., Hirakawa, H., Ishida, T., Hayashi, S., Kurebayashi, J., Sasano, H., Suzuki, T.	Intratumoral estrogen concentration and expression of estrogen-induced genes in male breast carcinoma: comparison with female breast carcinoma.	Hormones and Cancer	4(1)	1-11	2012
Gohno, T., Seino, Y., Hanamura, T., Niwa, T., Matsumoto, M., Yaegashi, N., Oba, H., Kurosumi, M., Takei, H., Yamaguchi, Y., Hayashi, S.	Individual transcription activity of estrogen receptors in primary breast cancer and its clinical significance.	Cancer Medicine	1(3)	328-337	2012
Suda, T., Oba, H., Takei, H., Kurosumi, M., Hayashi, S., Yamaguchi, Y.	ER-activating ability of breast cancer stromal fibroblasts is regulated independently of alteration of TP53 and PTEN tumor suppressor genes.	Biochem. Biophys. Res. Commun	428	259-263	2012

Transforming mutations of RAC guanosine triphosphatases in human cancers

Masahito Kawazu^a, Toshihide Ueno^b, Kenji Kontani^c, Yoshitaka Ogita^c, Mizuo Ando^a, Kazutaka Fukumura^a, Azusa Yamato^b, Manabu Soda^b, Kengo Takeuchi^d, Yoshio Miki^e, Hiroyuki Yamaguchi^a, Takahiko Yasuda^{a,f}, Tomoki Naoe^f, Yoshihiro Yamashita^b, Toshiaki Katada^c, Young Lim Choi^a, and Hiroyuki Mano^{a,b,g,1}

^aDepartment of Medical Genomics, Graduate School of Medicine, University of Tokyo, Tokyo 113-0033, Japan; ^bDivision of Functional Genomics, Jichi Medical University, Tochigi 329-0498, Japan; ^cDepartment of Physiological Chemistry, Graduate School of Pharmaceutical Sciences, University of Tokyo, Tokyo 113-0033, Japan; ^dPathology Project for Molecular Targets, The Cancer Institute, Japanese Foundation for Cancer Research, Tokyo 135-8550, Japan; ^eDepartment of Genetic Diagnosis, The Cancer Institute, Japanese Foundation for Cancer Research, Tokyo 135-8550, Japan; ^fDepartment of Hematology and Oncology, Nagoya University Graduate School of Medicine, Nagoya 466-8550, Japan; and ^gCore Research for Evolutional Science and Technology, Japan Science and Technology Agency, Saitama 332-0012, Japan

Edited by Shuh Narumiya, Kyoto University Faculty of Medicine, Kyoto, Japan, and accepted by the Editorial Board January 9, 2013 (received for review September 22, 2012)

Members of the RAS superfamily of small guanosine triphosphatases (GTPases) transition between GDP-bound, inactive and GTP-bound, active states and thereby function as binary switches in the regulation of various cellular activities. Whereas HRAS, NRAS, and KRAS frequently acquire transforming missense mutations in human cancer, little is known of the oncogenic roles of other small GTPases, including Ras-related C3 botulinum toxin substrate (RAC) proteins. We show that the human sarcoma cell line HT1080 harbors both NRAS(Q61K) and RAC1(N92I) mutant proteins. Whereas both of these mutants were able to transform fibroblasts, knock-down experiments indicated that RAC1(N92I) may be the essential growth driver for this cell line. Screening for RAC1, RAC2, or RAC3 mutations in cell lines and public databases identified several missense mutations for RAC1 and RAC2, with some of the mutant proteins, including RAC1(P29S), RAC1(C157Y), RAC2(P29L), and RAC2(P29Q), being found to be activated and transforming. P29S, N92I, and C157Y mutants of RAC1 were shown to exist preferentially in the GTP-bound state as a result of a rapid transition from the GDP-bound state, rather than as a result of a reduced intrinsic GTPase activity. Activating mutations of RAC GTPases were thus found in a wide variety of human cancers at a low frequency; however, given their marked transforming ability, the mutant proteins are potential targets for the development of new therapeutic agents.

oncogene | resequencing

The identification of transforming proteins and the development of agents that target them have markedly influenced the treatment and improved the prognosis of individuals with cancer. Chronic myeloid leukemia (CML), for example, has been shown to result from the growth-promoting activity of the fusion tyrosine kinase breakpoint cluster region-Abelson murine leukemia viral oncogene homolog 1 (BCR-ABL1), and treatment with a specific ABL1 inhibitor, imatinib mesylate, has increased the 5-y survival rate of individuals with CML to almost 90% (1). Similarly, the fusion of echinoderm microtubule associated protein like 4 gene (*EML4*) to anaplastic lymphoma receptor tyrosine kinase (*ALK*) is responsible for a subset of non-small-cell lung cancer cases (2), and therapy targeted to *EML4*-*ALK* kinase activity has greatly improved the progression-free survival of affected individuals compared with that achieved with conventional chemotherapies (3). Therapies that target essential growth drivers in human cancers are thus among the most effective treatments for these intractable disorders.

V-Ki-ras2 Kirsten rat sarcoma viral oncogene homolog (KRAS), v-Ha-ras Harvey rat sarcoma viral oncogene homolog (HRAS), and neuroblastoma RAS viral (v-ras) oncogene homolog (NRAS) are the founding members of the rat sarcoma (RAS) superfamily of small guanosine triphosphatases (GTPases)

that is known to comprise >150 members in humans (4). Five subgroups of these small GTPases have been identified and designated as the RAS; ras homolog family member (RHO); RAB1A, member RAS oncogene family (RAB); RAN, member RAS oncogene family (RAN); and ADP-ribosylation factor (ARF) families. All small GTPases function as binary switches that transition between GDP-bound, inactive and GTP-bound, active forms and thereby contribute to intracellular signaling that underlies a wide array of cellular activities, including cell proliferation, differentiation, survival, motility, and transformation (5). Somatic point mutations that activate KRAS, HRAS, or NRAS have been identified in a variety of human tumors, with KRAS being the most frequently activated oncoprotein in humans. Somatic activating mutations of KRAS are thus present in >90% of pancreatic adenocarcinomas, for example (6). Surprisingly, however, mutational activation of small GTPases other than KRAS, HRAS, and NRAS has not been widely reported.

Ras-related C3 botulinum toxin substrate (RAC) 1, RAC2, and RAC3 belong to the RHO family of small GTPases (7). RAC proteins orchestrate actin polymerization, and their activation induces the formation of membrane ruffles and lamellipodia (8), which play essential roles in the maintenance of cell morphology and in cell migration. Accumulating evidence also indicates that RAC proteins function as key hubs of intracellular signaling that underlies cell transformation. RAC1, for example, serves as an essential downstream component of the signaling pathway by which oncogenic RAS induces cell transformation, and artificial introduction of an amino acid substitution (G12V) into RAC1 renders it oncogenic (9). Furthermore, suppression of RAC1 activity induces apoptosis in glioma cells (10), and loss of *RAC1* or *RAC2* results in a marked delay in the development of BCR-ABL1-driven myeloproliferative disorder (11). Despite such important roles of RAC proteins in cancer, somatic transforming mutations of these proteins have not been identified in cancer specimens.

We have now discovered a mutant form of RAC1 with the amino acid substitution N92I in a human sarcoma cell line, HT1080, and have found that this mutation renders RAC1 constitutively active and highly oncogenic. Even though HT1080 cells also harbor the NRAS(Q61K) oncoprotein, RAC1(N92I) is the essential growth driver in this cell line, given that RNA interference (RNAi)-

Author contributions: M.K. and H.M. designed research; M.K., T.U., K.K., Y.O., M.A., K.F., A.Y., M.S., K.T., Y.M., H.Y., T.Y., T.N., Y.Y., T.K., and Y.L.C. performed research; M.K., T.U., K.K., Y.O., K.T., T.N., T.K., Y.L.C., and H.M. analyzed data; and H.M. wrote the paper.

The authors declare no conflict of interest.

This article is a PNAS Direct Submission. S.N. is a guest editor invited by the Editorial Board.

¹To whom correspondence should be addressed. E-mail: hmano@m.u-tokyo.ac.jp.

This article contains supporting information online at www.pnas.org/lookup/suppl/doi:10.1073/pnas.1216141110/-DCSupplemental.

mediated knockdown of RAC1(N92I) markedly suppressed cell growth. Further screening for *RAC1*, *RAC2*, and *RAC3* mutations among cancer cell lines as well as public databases identified additional transforming mutations of RAC1 and RAC2. Our data thus reveal oncogenic amino acid substitutions for the RAC subfamily of small GTPases in human cancer.

Results

Discovery of the RAC1(N92I) Oncoprotein. To identify transforming genes in the fibrosarcoma cell line HT1080 (12), we isolated cDNAs for cancer-related genes ($n = 906$) from HT1080 cells and subjected them to deep sequencing with the Genome Analyzer IIx (GAIIx) system. Quality filtering of the 92,025,739 reads obtained yielded 45,325,377 unique reads that mapped to 843 (93.0%) of the 906 target genes. The mean read coverage for the 843 genes was 495 \times per nucleotide, and $\geq 70\%$ of the captured regions for 568 genes were read at $\geq 10\times$ coverage.

Screening for nonsynonymous mutations in the data set with the use of our computational pipeline (13) revealed a total of five missense mutations with a threshold of $\geq 30\times$ coverage and a $\geq 30\%$ mutation ratio (Table S1). One of these mutations, a heterozygous missense mutation of *NRAS* that results in a Gln-

to-Lys substitution at amino acid position 61 (Q61K), was described previously in this cell line (14) and is the most frequent transforming mutation of *NRAS* (5). We also discovered a missense mutation in another small GTPase, RAC1 (Fig. S1 and Table S1). An A-to-T transversion at position 516 of human *RAC1* cDNA (GenBank accession no. NM_006908.4), resulting in an Asn-to-Ile substitution at position 92 of the encoded protein, was thus identified in 11,525 (47.5%) of the 24,238 total reads covering this position.

To examine the transforming potential of RAC1(N92I), we infected mouse 3T3 fibroblasts and MCF10A human mammary epithelial cells (15) with a retrovirus encoding wild-type or N92I mutant form of human RAC1 and then seeded the cells in soft agar for evaluation of anchorage-independent growth. Neither 3T3 nor MCF10A cells expressing wild-type RAC1 grew in soft agar (Fig. 1A), indicating the lack of transforming potential of RAC1. In contrast, the cells expressing RAC1(N92I) readily grew in soft agar (Fig. 1A), showing that this RAC1 mutant confers the property of anchorage-independent growth on both 3T3 and MCF10A cells. We also confirmed the transforming potential of an artificial mutant of RAC1, RAC1(G12V) (8),

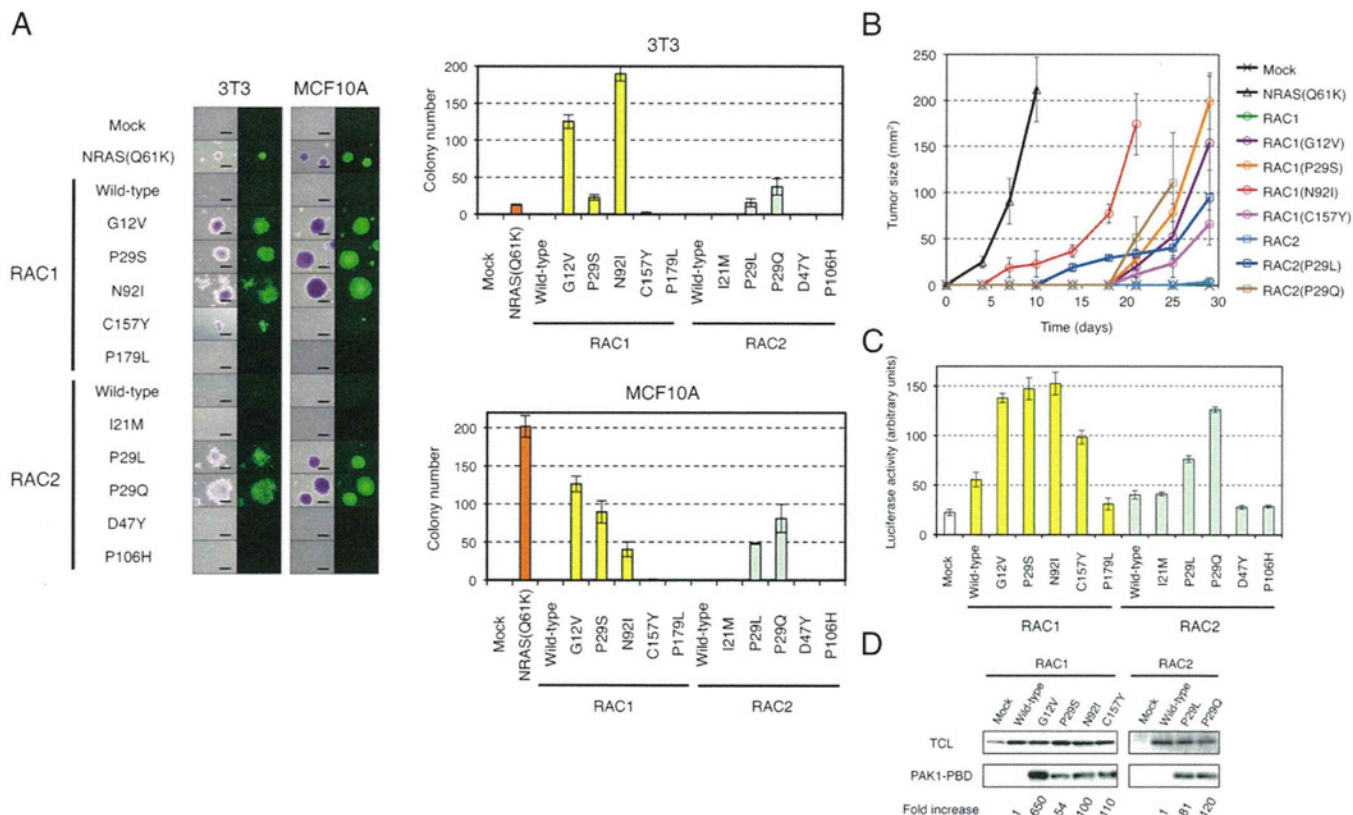


Fig. 1. Transforming potential of RAC1 and RAC2 mutants. (A) 3T3 or MCF10A cells were infected with recombinant retroviruses encoding enhanced green fluorescent protein (EGFP) as well as wild-type or mutant forms of RAC1 or RAC2 and were then assayed for anchorage-independent growth in vitro under the presence of 10% (vol/vol) FBS. After 14 d (3T3) or 20 d (MCF10A) of culture, the cells were stained with crystal violet and examined by conventional microscopy (Left: left image of each pair), and they were monitored for EGFP expression by fluorescence microscopy (Left: right image of each pair). (Scale bars, 0.5 mm.) The numbers of cell colonies were also determined as means \pm SD from three independent experiments (Right). (B) 3T3 cells expressing wild-type or mutant forms of RAC1 or RAC2 were injected s.c. into the shoulder of nude mice, and the size of the resulting tumors [(length \times width)/2] was determined at the indicated times thereafter. Tumor size for 3T3 expressing NRAS(Q61K) was similarly monitored. Data are means \pm SD for tumors at four injection sites. (C) HEK293T cells were transfected with expression vectors for wild-type or mutant forms of RAC1 or RAC2 together with the SRE.L reporter plasmid and pGL-TK. The activity of firefly luciferase in cell lysates was then measured and normalized by that of *Renilla* luciferase. Data are means \pm SD from three independent experiments. (D) Lysates of 3T3 cells expressing wild-type or mutant forms of RAC1 or RAC2 were subjected to a pull-down assay with PAK1-PBD. The precipitated proteins as well as the total cell lysates were then subjected to immunoblot analysis with antibodies to RAC1 or to RAC2. The relative amounts of pulled-down RAC proteins compared with their corresponding expression levels in total cell lysate were normalized to that of wild-type RAC1 (for the RAC1 mutants) or RAC2 (for the RAC2 mutants) and are shown at the bottom.

which harbors an amino acid substitution corresponding to that of the oncogenic G12V mutant form of RAS proteins.

Other Transforming Mutations of RAC1 and RAC2. We next searched for other transforming mutations of RAC proteins. Human RAC1, RAC2 (GenBank accession no. NM_002872.3), and RAC3 (GenBank accession no. NM_005052.2) cDNAs were isolated from 40 cancer cell lines (Table S2), and their nucleotide sequences were determined by Sanger sequencing, resulting in the discovery of RAC1(P29S), RAC2(P29Q), and RAC2(P29L) in the breast cancer cell line MDA-MB-157, the CML cell line KCL-22, and the breast cancer cell line HCC1143, respectively (Fig. S1 and Table S3). Further searching for RAC1, RAC2, and RAC3 mutations in the COSMIC database of cancer genome mutations (Release V59; <http://cancer.sanger.ac.uk/cancergenome/projects/cosmic>) revealed various amino acid substitutions detected in human tumors, namely RAC1(P29S), RAC1(C157Y), RAC1(P179L), RAC2(I21M), RAC2(P29L), RAC2(D47Y), and RAC2(P106H) (Table S3). Importantly, all of these RAC1 and RAC2 mutations identified in clinical specimens were confirmed to be somatic, given that the corresponding mutations were absent in the genome of paired normal cells.

To examine the transforming potential of these various RAC1 and RAC2 mutants, we expressed each protein in 3T3 and MCF10A cells and evaluated anchorage-independent growth. Whereas the wild-type form of RAC2 did not transform 3T3 or MCF10A cells, growth in soft agar was apparent for 3T3 cells expressing RAC1 (P29S), RAC1(C157Y), RAC2(P29L), or RAC2(P29Q), but not for those expressing RAC1(P179L), RAC2(I21M), RAC2(D47Y), or RAC2(P106H) (Fig. 1A). Of interest, colony number in the assay varied substantially in a manner dependent on the type of amino acid substitution as well as on cell type. RAC1(C157Y), for example, yielded fewer colonies in soft agar compared with the other transforming mutants. Furthermore, RAC1(P29S), which was identified in a breast cancer cell line, generated a larger number of colonies with MCF10A cells than with 3T3 cells. Conversely, RAC1(N92I), which was identified in a fibrosarcoma cell line, yielded a larger number of colonies with 3T3 cells than with MCF10A cells. The oncogenic activity of RAC1(P29S), RAC1(N92I), RAC1(C157Y), RAC2(P29L), and RAC2(P29Q) mutants was further confirmed with a tumorigenicity assay in nude mice (Fig. 1B), with the activity of RAC1(N92I) being the most pronounced with regard to the transformation of 3T3 cells in this assay.

The colony number in soft agar for 3T3 cells expressing NRAS(Q61K) was fewer than that for the cells expressing oncogenic RAC1 or RAC2 mutants (Fig. 1A), whereas expression of these small GTPases was readily confirmed in 3T3 (Fig. S2). Interestingly,

s.c. tumors from the same 3T3 cells expressing NRAS(Q61K) grew more rapidly than tumors expressing the RAC1/RAC2 mutants (Fig. 1B), indicating that the measured intensity of the transforming potential of GTPases may vary in a dependent manner on assay systems.

To examine whether such oncogenic potential is linked directly to the activation of RAC1 or RAC2, we investigated the activity of the mutant proteins with the use of a luciferase reporter plasmid that selectively responds to intracellular signaling evoked by RHO family GTPases (16). In concordance with the data from the soft agar and tumorigenicity assays, only the transforming mutants of RAC1 and RAC2 yielded a substantial level of luciferase activity in transfected HEK293T cells (Fig. 1C).

Activated RAC1 or RAC2 would be expected to be loaded with GTP. We therefore examined the GTP-binding status of the RAC1 and RAC2 oncoproteins with the use of a pull-down assay based on the p21-binding domain (PBD) of PAK1. All of the transforming RAC1 and RAC2 mutants were found to exist preferentially in the GTP-bound state (Fig. 1D), indicative of their constitutive activation. Furthermore, these RAC1 and RAC2 mutants induced marked reorganization of the actin cytoskeleton in 3T3 cells, resulting in the accumulation of polymerized actin in ruffles at the plasma membrane (Fig. 2).

RAC1 and RAC2 as Therapeutic Targets. Given that NRAS(Q61K) is also known to transform 3T3 cells (17) (Fig. 1A), our data show that HT1080 cells harbor two independent oncogenic GTPases. We therefore examined whether RAC1(N92I) or NRAS(Q61K) is the principal growth driver in this sarcoma cell line. Among several small interfering RNAs (siRNAs) designed to attenuate the expression of RAC1 or NRAS, we selected two independent siRNAs that specifically target each mRNA (Fig. 3A). Whereas transfection of HT1080 cells with either NRAS siRNA resulted in a moderate inhibition of cell proliferation under the presence of 10% (vol/vol) FBS, that with either RAC1 siRNA almost blocked cell growth (Fig. 3B). Transfection with an NRAS siRNA in addition to either RAC1 siRNA did not result in an additional effect on cell proliferation (Fig. 3B). Similar data were observed in a culture with 1% (vol/vol) FBS (Fig. S3A) or under FBS-free conditions (Fig. S3B). To further examine the effects of silencing RAC1/NRAS, we quantitated cell cycle distribution of HT1080 transfected with siRNAs against either RAC1 or NRAS. As shown in Fig. S4A, DNA synthesis was equally suppressed by the knockdown of RAC1 or NRAS. Interestingly, however, CASP3/CASP7 activity (a surrogate marker for apoptosis) was markedly induced only by RAC1 depletion (Fig. S4B). Therefore, RAC proteins are likely to provide RAS-independent cell survival

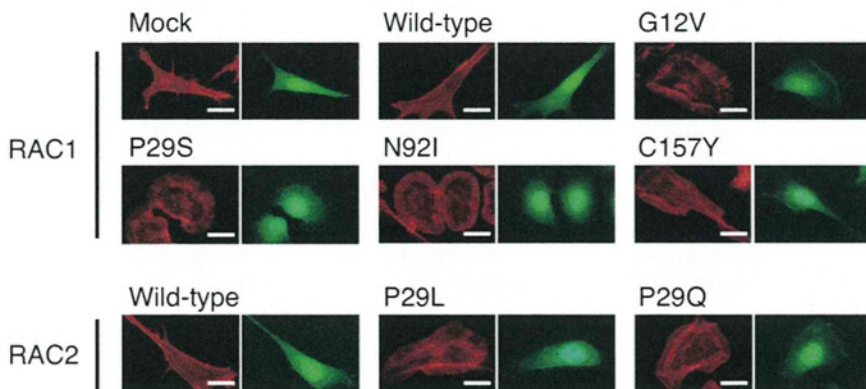


Fig. 2. Actin reorganization induced by the RAC1/RAC2 mutants. 3T3 cells infected with retroviruses encoding enhanced green fluorescent protein (EGFP) as well as wild-type or mutant forms of RAC1 or RAC2 were stained with Alexa Fluor 594-labeled phalloidin to visualize actin organization (Left image of each pair). The same cells were also examined for EGFP fluorescence (Right image of each pair). (Scale bars, 20 μ m.)

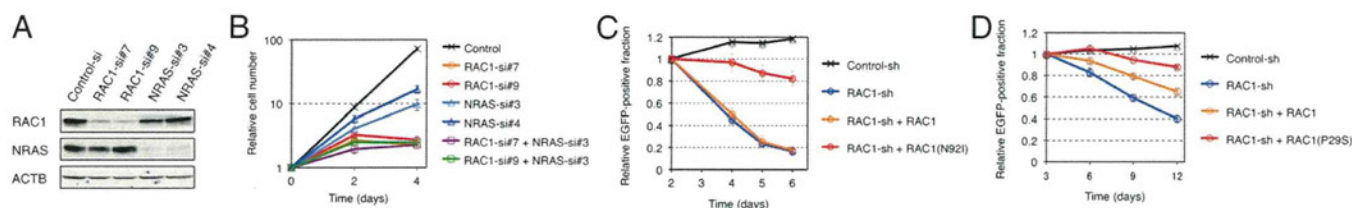


Fig. 3. Oncogenic RAC proteins as therapeutic targets. (A) HT1080 cells were transfected with control, RAC1, or NRAS siRNAs; lysed; and subjected to immunoblot analysis with antibodies to RAC1, NRAS, or ACTB (loading control). (B) HT1080 cells were transfected with control, RAC1, or NRAS siRNAs, as indicated, and cultured under the presence of 10% (vol/vol) FBS. Cell number was counted at the indicated times after the onset of transfection. Data are means \pm SD from three independent experiments. (C) HT1080 cells were infected with a retrovirus encoding green fluorescent protein (EGFP) as well as a control or RAC1 shRNA. They were also infected with a retrovirus encoding shRNA-resistant wild-type RAC1 or RAC1(N92I), as indicated. The number of EGFP-positive cells was determined by flow cytometry after culture of the cells for the indicated times, and the size of the EGFP-positive fraction relative to that at 2 d was calculated. Data are means \pm SD from three independent experiments. (D) MDA-MB-157 cells were infected with a retrovirus encoding EGFP as well as a control or RAC1 shRNA. They were also infected with a retrovirus encoding shRNA-resistant wild-type RAC1 or RAC1(P29S), as indicated. The number of EGFP-positive cells was determined by flow cytometry after culture of the cells for the indicated times, and the size of the EGFP-positive fraction relative to that at 3 d was calculated. Data are means \pm SD from three independent experiments.

signals, which is supported by the fact that, even under FBS-free conditions, RAC1 depletion has more antiproliferative effects in HT1080 than NRAS depletion (Fig. S3B). These data show that active RAC1 may be the essential growth driver in HT1080 cells and is therefore a potential therapeutic target. Furthermore, our data suggest that oncogenic RAS proteins may require additional transforming hits to give rise to full-blown cancer.

We next infected HT1080 cells with a retrovirus expressing a short hairpin RNA (shRNA) targeted to RAC1 mRNA. Expression of the RAC1 shRNA markedly suppressed cell growth, whereas restoration of shRNA-resistant RAC1(N92I) expression reversed this effect (Fig. 3C and Fig. S5), showing that the effect of the RAC1 shRNA was not an off-target artifact. Forced expression

of shRNA-resistant wild-type RAC1 failed to reverse the inhibitory effect of the RAC1 shRNA on cell growth, indicating that growth suppression by the shRNA was due to depletion of the N92I mutant, not to that of the wild-type protein. We performed similar experiments with the breast cancer cell line MDA-MB-157, which harbors RAC1(P29S). Again, the RAC1 shRNA inhibited cell growth, and this effect was reversed to a larger extent by restoration of the expression of shRNA-resistant RAC1(P29S) than by forced expression of the wild-type protein (Fig. 3D and Fig. S5).

RAC1(P29S), RAC1(N92I), and RAC1(C157Y) Are Rapid-Cycling Mutants. Oncogenic mutations at G12, G13, or Q61 of RAS proteins found in human tumors reduce the intrinsic GTPase activity of these

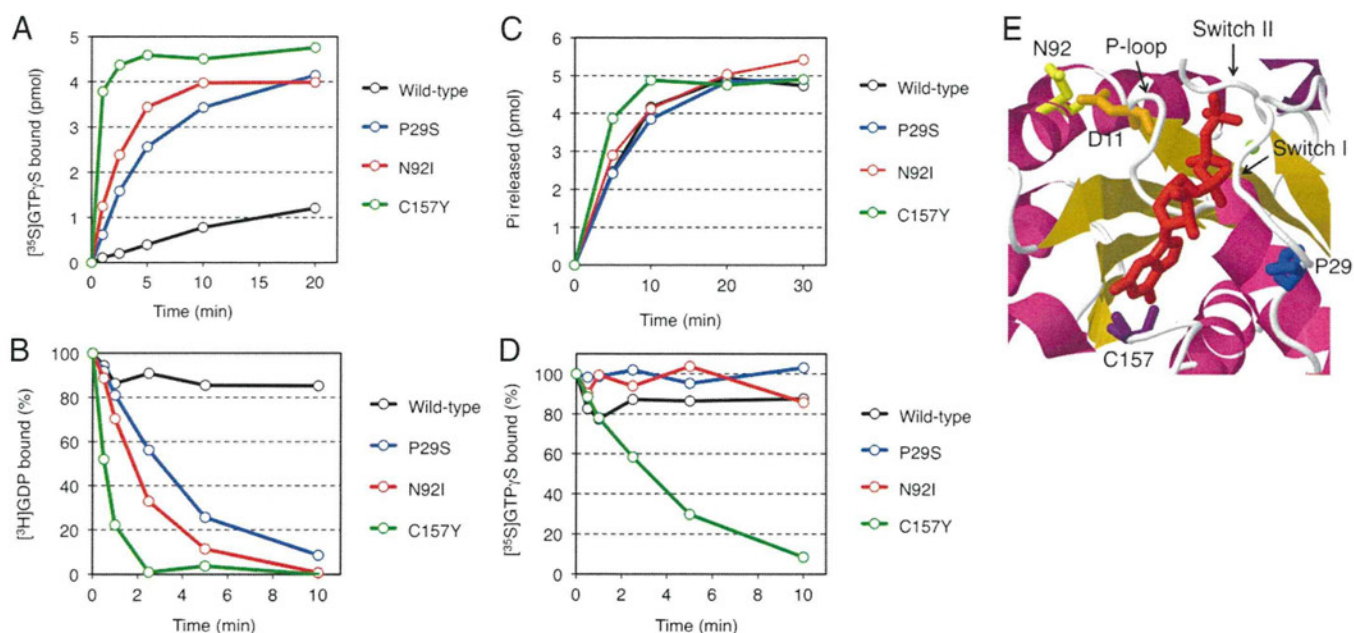


Fig. 4. Biochemical properties of RAC1 mutants. (A) Bacterially expressed and purified proteins of the wild-type, P29S, N92I, or C157Y mutant of RAC1 (5 pmol each) were incubated with [35 S]GTP γ S in the presence of 0.8 mM Mg $^{2+}$, and the amounts of [35 S]GTP γ S-bound proteins were determined at the indicated times. (B) [3 H]GDP dissociation from [3 H]GDP-bound RAC1 proteins was initiated by the addition of unlabeled GTP γ S in the presence of 0.8 mM Mg $^{2+}$, and the amounts of [3 H]GDP-bound proteins were determined at the indicated times. (C) RAC1 proteins were preloaded with [γ - 32 P] GTP, and then GTP hydrolysis reactions were initiated by the addition of unlabeled GTP in the presence of 0.8 mM Mg $^{2+}$. Pi released from the proteins was isolated and measured at the indicated times. (D) [35 S]GTP γ S dissociation from [35 S]GTP γ S-bound RAC1 proteins was initiated by the addition of unlabeled GTP γ S in the presence of 0.8 mM Mg $^{2+}$, and the amounts of [35 S]GTP γ S-bound proteins were determined at the indicated times. (E) Schematic representation of the structure of the GTP-binding pocket of human RAC1 (ID 1mh1 in the Protein Data Bank; www.pdb.org) with α -helices and β -sheets shown in magenta and orange, respectively. The GTP analog guanosine 5'-(β,γ -imido)-triphosphate (GppNp) and Mg $^{2+}$ are depicted in red and green, respectively. D11, P29, N92, and C157 amino acid residues are in orange, blue, yellow and purple, respectively. The positions of switch I and switch II regions and the P-loop are also indicated.

proteins and thereby maintain them in the GTP-bound state (18, 19). On the other hand, an artificial F28L substitution in HRAS or the RHO family protein Cdc42Hs was shown to confer constitutive activity by accelerating the transition from the GDP-bound to the GTP-bound state without the involvement of an exogenous guanine nucleotide exchange factor (GEF) (20, 21).

To determine how transforming mutations of RAC1 results in constitutive activation of these proteins, we examined their affinity for GTP and GDP. Compared with wild-type RAC1, all of RAC1(P29S), RAC1(N92I), and RAC1(C157Y) was found to bind GTP γ S (nonhydrolyzable GTP analog) rapidly *in vitro*, even without the addition of a GEF protein (Fig. 4A). Likewise, the dissociation of GDP from the mutant forms of RAC1 was greatly accelerated (Fig. 4B). On the other hand, the intrinsic GTPase activity of these mutants was similar to (for P29S and N92I) or slightly higher (for C157Y) than that of the wild-type protein (Fig. 4C). These data thus indicated that, in contrast to transforming RAS mutants associated with human cancer, RAC1 (P29S), RAC1(N92I), and RAC1(C157Y) are fast-cycling mutants, for which the probability of being in the GTP-bound state is increased as the result of an increased rate of GDP dissociation, rather than as the result of a loss of GTPase activity.

Interestingly, dissociation of GTP γ S was also accelerated only for RAC1(C157Y), but not for the wild-type, P29S, or N92I form of RAC1 (Fig. 4D). Thus, RAC1(C157Y) is a unique mutant in that both association and dissociation for GTP are accelerated, which may provide the molecular basis for its modest transforming potential compared with that of RAC1(P29S) or RAC1(N92I) (Fig. 1).

In the 3D structure of RAC1 (Fig. 4E), P29 is located in the switch I region, whereas C157 is positioned adjacent to the guanine ring of bound GTP. Substitution of these residues would thus likely affect the affinity of the protein for GDP or GTP (Fig. S6), a phenomenon that has been demonstrated recently for RAC1 (P29S) (22). In contrast, N92 is located distant from the binding pocket for GDP/GTP, and so the structural mechanism by which the N92I substitution renders RAC1 constitutively active remains elusive (Fig. 4E and Fig. S6). Residue N92 is located close to D11 in the P-loop of RAC1, however (Fig. 4E and Fig. S7), and substitution with isoleucine at this position would abolish the interaction between the amino group of N92 and the carboxyl group of D11. It is thus possible that the N92I mutation affects the binding of GDP/GTP through an effect on the P-loop.

Discussion

We have here demonstrated the transforming potential of mutated RAC proteins. Our analysis of cell lines resulted in the identification of transforming mutants of RAC1 and RAC2, namely RAC1(N92I) and RAC2(P29Q), and we also revealed the transforming potential of the RAC1(P29S), RAC1(C157Y), and RAC2(P29L) mutants deposited the COSMIC database of cancer genome mutations (Release V59; <http://cancer.sanger.ac.uk/cancergenome/projects/cosmic>) (Table S3). In contrast, the soft agar assay did not reveal a transforming potential of the RAC1(P179L), RAC2(I21M), RAC2(D47Y), or RAC2(P106H) mutants found in the database, suggesting a possibility that they are “passenger mutations.” It may also be possible, however, that these mutants may still contribute to cancer development by modifying tumor properties (such as metastasis ability), given that they were somatically acquired and clonally selected in cancer.

An important finding of our study was that the oncogenic effects of RAC1(N92I) may be more pronounced than those of NRAS(Q61K), at least with regard to survival signals in HT1080 cells (Fig. 3B). It should be noted, however, that HT1080 expresses RAC1 almost exclusively among the RAC family proteins, whereas HRAS and KRAS are weakly expressed in addition to NRAS (Fig. S8). It is thus possible that the effects of NRAS

knockdown in Fig. 3B may be partly complemented by the residual HRAS/KRAS proteins.

Paterson et al. previously isolated NRAS-attenuated subclones of HT1080 after treatment with an alkylating reagent (*N*-methyl-*N'*-nitro-*N*-nitrosoguanidine) and a subsequent culture with 5-fluorodeoxyuridine and 1- β -D-arabinofuranosylcytosine (23). Such subclones had a flat cell shape and a reduced ability for anchorage-independent growth. Likewise, we noted that transfection with NRAS siRNAs renders HT1080 a flatter shape (Fig. S9). As demonstrated in Fig. 3B and by Paterson et al. (23), however, such NRAS-depleted HT1080 was still viable and kept proliferation *in vitro*, suggesting the presence of other oncogene(s) in addition to NRAS(Q61K). Therefore, NRAS(Q61K) and RAC1(N92I) are likely to cooperate to fully transform this fibrosarcoma.

Regarding the coexistence of mutations within RAC family proteins and RAS-RAF-MAPK proteins, two studies independently reported recurrent P29S mutation of RAC1 in melanoma during the preparation of this article (22, 24). Of note, BRAF (V600E) was also detected in four of six and in two of seven of the RAC mutation-positive melanomas, respectively. These observations, together with our findings with HT1080 cells, thus indicate that activating mutations of RAC1 and those of the RAS-RAF-signaling pathway are not mutually exclusive.

Members of the RAC subfamily of GTPases show a high level of sequence identity in humans. The amino acid sequence of RAC1 is thus 92% identical to that of RAC2 or RAC3. Furthermore, all of the amino acid residues of RAC1 or RAC2 found to be mutated in cancer (Table S3) are completely conserved among RAC1, RAC2, and RAC3. Thus, transforming RAC3 mutants with similar nonsynonymous mutations may also exist in human cancer, although such mutations were not detected in the current screening. Of interest, none of the frequent mutation sites in RAS family proteins (G12, G13, and Q61) were found to be affected in RAC1 or RAC2, although an artificial G12V mutant of RAC1 did manifest constitutive GTP loading and transforming potential. Given that RAC proteins perform intracellular functions (such as orchestration of the actin cytoskeleton) that are distinct from those of RAS family members, RAC-driven activation of specific intracellular pathways may be advantageous for cancer development *in vivo*.

Given that we detected activation mutations of RAC1 or RAC2 in cell lines from sarcoma (HT1080), triple-negative breast cancer (MDA-MB-157 and HCC1143), and the blast crisis stage of CML (KCL-22), we performed deep sequencing of RAC1, RAC2, and RAC3 cDNAs with GAIIX for specimens of triple-negative breast cancer ($n = 66$), of RAC1 and RAC2 cDNAs for specimens of CML in blast crisis ($n = 43$), and of BCR-ABL1-positive acute lymphoblastic leukemia ($n = 31$), as well as of RAC1 cDNAs for specimens of sarcoma ($n = 53$). We failed, however, to detect any nonsynonymous mutations among these RAC cDNAs.

Our results have shown that RAC proteins have the potential to become oncogenic through amino acid substitution in a wide array of cancers. Although such RAC mutations may occur at a low frequency, the recent studies of Krauthammer et al. (22) and Hodis et al. (24) suggest that they may be enriched in melanoma (~5%). Importantly, given that HT1080 cells are highly addicted to the increased activity of RAC1(N92I), the targeting of oncogenic RAC proteins or their downstream effectors with small compounds or RNAi may prove to be an effective approach to the treatment of cancer harboring such oncoproteins.

Materials and Methods

The human fibrosarcoma cell line HT1080 was obtained from American Type Culture Collection, and subjected to deep sequencing with GAIIX. Recombinant retrovirus expressing the wild-type or mutant forms of RAC1 or RAC2 was used to infect mouse 3T3 fibroblasts to examine its transforming potential. Detailed information for cDNA resequencing, transformation assays, biochemical analysis of RAC proteins, and RNAi are detailed in *SI Materials and Methods*.

ACKNOWLEDGMENTS. This study was supported in part by a grant for Research on Human Genome Tailor-Made from the Ministry of Health, Labor, and Welfare of Japan; Grants-in-Aid for Scientific Research (B) from

the Japan Society for the Promotion of Science; and grants from The Yasuda Medical Foundation, The Sagawa Foundation for Promotion of Cancer Research, and The Mitsubishi Foundation.

1. Druker BJ, et al.; IRIS Investigators (2006) Five-year follow-up of patients receiving imatinib for chronic myeloid leukemia. *N Engl J Med* 355(23):2408–2417.
2. Soda M, et al. (2007) Identification of the transforming *EML4-ALK* fusion gene in non-small-cell lung cancer. *Nature* 448(7153):561–566.
3. Shaw AT, et al. (2011) Effect of crizotinib on overall survival in patients with advanced non-small-cell lung cancer harbouring *ALK* gene rearrangement: A retrospective analysis. *Lancet Oncol* 12(11):1004–1012.
4. Colicelli J (2004) Human *RAS* superfamily proteins and related GTPases. *Sci STKE* 2004(250):RE13.
5. Cox AD, Der CJ (2010) Ras history: The saga continues. *Small GTPases* 1(1):2–27.
6. Jaffee EM, Hruban RH, Canto M, Kern SE (2002) Focus on pancreas cancer. *Cancer Cell* 2(1):25–28.
7. Wertheimer E, et al. (2012) Rac signaling in breast cancer: A tale of GEFs and GAPs. *Cell Signal* 24(2):353–362.
8. Ridley AJ, Paterson HF, Johnston CL, Diekmann D, Hall A (1992) The small GTP-binding protein *rac* regulates growth factor-induced membrane ruffling. *Cell* 70(3):401–410.
9. Qiu RG, Chen J, Kirn D, McCormick F, Symons M (1995) An essential role for *Rac* in Ras transformation. *Nature* 374(6521):457–459.
10. Senger DL, et al. (2002) Suppression of *Rac* activity induces apoptosis of human glioma cells but not normal human astrocytes. *Cancer Res* 62(7):2131–2140.
11. Thomas EK, et al. (2007) *Rac* guanosine triphosphatases represent integrating molecular therapeutic targets for BCR-ABL-induced myeloproliferative disease. *Cancer Cell* 12(5):467–478.
12. Rasheed S, Nelson-Rees WA, Toth EM, Arnstein P, Gardner MB (1974) Characterization of a newly derived human sarcoma cell line (HT-1080). *Cancer* 33(4):1027–1033.
13. Ueno T, et al. (2012) High-throughput resequencing of target-captured cDNA in cancer cells. *Cancer Sci* 103(1):131–135.
14. Hall A, Marshall CJ, Spurr NK, Weiss RA (1983) Identification of transforming gene in two human sarcoma cell lines as a new member of the *ras* gene family located on chromosome 1. *Nature* 303(5916):396–400.
15. Debnath J, Muthuswamy SK, Brugge JS (2003) Morphogenesis and oncogenesis of MCF-10A mammary epithelial acini grown in three-dimensional basement membrane cultures. *Methods* 30(3):256–268.
16. Hill CS, Wynne J, Treisman R (1995) The Rho family GTPases *RhoA*, *Rac1*, and *CDC42Hs* regulate transcriptional activation by *SRF*. *Cell* 81(7):1159–1170.
17. Marshall CJ, Hall A, Weiss RA (1982) A transforming gene present in human sarcoma cell lines. *Nature* 299(5879):171–173.
18. Adari H, Lowy DR, Willumsen BM, Der CJ, McCormick F (1988) Guanosine triphosphatase activating protein (GAP) interacts with the p21 *ras* effector binding domain. *Science* 240(4851):518–521.
19. Calés C, Hancock JF, Marshall CJ, Hall A (1988) The cytoplasmic protein GAP is implicated as the target for regulation by the *ras* gene product. *Nature* 332(6164):548–551.
20. Reinstein J, Schlichting I, Frech M, Goody RS, Wittinghofer A (1991) p21 with a phenylalanine 28→leucine mutation reacts normally with the GTPase activating protein GAP but nevertheless has transforming properties. *J Biol Chem* 266(26):17700–17706.
21. Lin R, Bagrodia S, Cerione R, Manor D (1997) A novel *Cdc42Hs* mutant induces cellular transformation. *Curr Biol* 7(10):794–797.
22. Krauthammer M, et al. (2012) Exome sequencing identifies recurrent somatic *RAC1* mutations in melanoma. *Nat Genet* 44(9):1006–1014.
23. Paterson H, et al. (1987) Activated *N-ras* controls the transformed phenotype of HT1080 human fibrosarcoma cells. *Cell* 51(5):803–812.
24. Hodis E, et al. (2012) A landscape of driver mutations in melanoma. *Cell* 150(2):251–263.

High level of miR-21, miR-10b, and miR-31 expression in bilateral vs. unilateral breast carcinomas

Aglaya G. Iyevleva · Ekatherina Sh. Kuligina ·
Nathalia V. Mitiushkina · Alexandr V. Togo ·
Yoshio Miki · Evgeny N. Imyanitov

Received: 23 June 2011 / Accepted: 18 October 2011 / Published online: 5 November 2011
© Springer Science+Business Media, LLC. 2011

Abstract We analyzed the expression of several microRNAs (miRs) implicated in breast cancer (BC) pathogenesis (miR-21, miR-10b, miR17-5p, miR-31, miR-155, miR-200c, miR-18a, miR-205, and miR-27a) in 80 breast carcinomas obtained from patients with bilateral BC (biBC) and 40 cases of unilateral BC (uBC). Unexpectedly, three miRs (miR-21, miR-10b and miR-31) demonstrated significantly higher level of expression in biBC vs. uBC ($P = 0.0001$, 0.00004 and 0.0002 , respectively). Increased contents of miR-21, miR-10b and miR-31 were observed in all categories of biBC tumors, i.e., in synchronous biBC as well as in first and second tumors from metachronous biBC cases. Synchronous biBC showed more similarity of miR expression profiles within pairs than the metachronous doublets ($P = 0.004$). This study suggests that bilateral breast tumors have somewhat distinct pattern of molecular events as compared to the unilateral disease.

Keywords microRNA · Bilateral breast cancer · Breast cancer predisposition

Introduction

Bilateral breast cancer (biBC) represents approximately 5% of total breast cancer (BC) incidence. biBC patients develop the same disease twice; therefore, they are particularly likely to have high level of genetic or non-genetic predisposition to BC [1]. Genotyping studies have revealed elevated incidence of BC-predisposing germ-line mutations in biBC patients; however, the inherited defects in *BRCA1*, *BRCA2*, *CHEK2*, and other known BC genes explain only a minority of biBC cases [2]. Causes of double BC occurrence in the mutation-negative BC patients remain largely unknown, and cannot be explained by the excess of canonical BC risk factors [1, 3, 4]. biBC and unilateral BCs (uBC) demonstrate similar distribution of clinical and morphological disease features. Synchronous biBC pairs often show a noticeable concordance of tumor histology, expression characteristics, and patterns of somatic mutations, which can be attributed to nearly identical natural histories of simultaneously arising neoplasms [5–8]. Metachronous biBCs share genetic background of the host; however, some essential circumstances of tumor development may differ between the first and second neoplasms. Age interval may contribute to dissimilarity of metachronous biBC, especially if the disease onsets are separated by menopause [5, 7, 8]. There is also a survival bias, which selects for metachronous contralateral BC only those patients whose first cancer behaved favorably, and thus provided sufficient time interval to develop the second disease [9]. In addition, adjuvant treatment of hormone-sensitive BC by tamoxifen or aromatase inhibitors prevents the progression of the estrogen receptor (ER)-positive and/or progesterone

A. G. Iyevleva · E. Sh. Kuligina · N. V. Mitiushkina ·
A. V. Togo · E. N. Imyanitov (✉)
Laboratory of Molecular Oncology, N. N. Petrov Institute
of Oncology, Pesochny-2, 197758 St.-Petersburg, Russia
e-mail: evgeny@imyanitov.spb.ru

A. G. Iyevleva · E. N. Imyanitov
Department of Medical Genetics, St.-Petersburg Pediatric
Medical Academy, St.-Petersburg, Russia

Y. Miki
Department of Genetic Diagnosis, Cancer Institute,
Japanese Foundation for Cancer Research, Tokyo, Japan

E. N. Imyanitov
Department of Oncology, St.-Petersburg Medical Academy
for Postgraduate Studies, St.-Petersburg, Russia

receptor (PR)-positive preneoplastic clones in the remaining breast, thus skewing the distribution of subsequent malignancies toward the receptor-negative variants [10]. Furthermore, some data indicate that as many as 10% of contralateral metachronous BC arise not because of naturally occurring factors but because of adverse effects of therapy applied against the first tumor. These iatrogenic carcinomas have completely distinct patterns of molecular abnormalities [11].

biBC molecular characteristics have already been described with respect to genomic abnormalities, *p53* mutations, oncogene amplifications, and expression of the subtype-specific markers [5, 6, 8, 9, 12]. The last decade brought into attention a novel class of molecules with a broad role in cancer development, i.e., microRNAs (miRs). miRs orchestrate the activity of multiple genes by binding to complementary sequences in the target mRNAs. Specific interaction between miR and corresponding mRNA prevents translation of the protein or leads to the degradation of the coding transcript [13, 14]. Several miRs have been implicated in different aspects of BC progression (Table 1). In this article, we present the results of expression analysis of BC-associated miRs in bilateral and unilateral breast carcinomas.

Materials and methods

This study included 80 tumors obtained from biBC patients and 40 randomly selected unilateral BC. biBC collection

included 27 tumor pairs (synchronous: 16; metachronous: 11) as well as 26 non-paired samples obtained from biBC patients. Clinical characteristics of the studied tumors are presented in Table 2.

Total RNA was isolated by a standard protocol [45]. Multiplex reverse transcription (RT) on miR templates was performed as described by Chen et al. [46]. Stem-loop RT primers are listed in Table 3. Each RT reaction was performed in a total volume of 20 μ l and contained 2 μ l total RNA, 0.5 nM each miR-specific primer, 1 unit RNase inhibitor, 50 units MMLV reverse transcriptase, 1 \times MMLV buffer, and 1 mM each dNTP. Pulsed RT reaction was used to increase RT efficiency and diminish possible non-specific interactions between primers for different miRs. The reaction conditions were as follows: 38 cycles at 16°C for 20 s, 42°C for 20 s, 50°C for 1 s with a final step of 85°C for 10 min. Negative controls included both samples without RNA template and preparations of genomic DNA.

Real-time PCR amplification was carried out on the Bio-Rad iCycler iQTM Real-Time PCR Detection System. All reactions were carried out in duplicate in a total volume of 10 μ l. Each reaction contained 1 μ l RT product, 0.35 unit Taq DNA polymerase, 1 \times PCR buffer (pH = 8.3), 3.0 mM MgCl₂, 200 μ M each dNTP, 200 nM forward primer, 20 nM universal reverse primer, and 400 nM specific TaqMan probe (Table 2). After initial activation of Taq polymerase at 95°C for 10 min, the reactions were run for 45 cycles at 95°C for 15 s and 62°C for 60 s.

Table 1 MicroRNAs implicated in breast cancer development

miR	Target cancer-related genes	Relevance to breast cancer	References
Oncogenes			
miR-21	<i>PDCD4</i> , <i>PTEN</i> , <i>TPM1</i> , <i>maspin</i> , <i>bcl2</i> , <i>TIMP3</i> , <i>ANP32A</i> , <i>SMARCA4</i> , <i>MARCKS</i>	Regulates apoptosis, cell proliferation, invasion and metastasis; overexpressed in BC; associated with aggressive course of the disease	[13–19]
miR-10b	<i>HOXD10</i> , <i>Tiam1</i>	Promotes metastasis; upregulated in metastatic BC	[20, 21]
miR-155	<i>RHOA</i> , <i>FOXO3a</i> , <i>SOCS1</i> , <i>SMAD5</i> , <i>SHIP1</i>	Overexpressed in BC, especially in hormone receptor-negative tumors; involved in epithelial-mesenchymal transition	[14, 22–27]
miR-27a	<i>FOXO1</i> , <i>ZBTB10</i> , <i>Myt1</i> , <i>Spry2</i> , <i>prohibitin</i>	Regulates estrogen signaling, cell cycle	[28–32]
Tumor suppressors			
miR-31	<i>FZD3</i> , <i>ITGA5</i> , <i>M-RIP</i> , <i>MMP16</i> , <i>RDX</i> , <i>RHOA</i> , <i>SATB2</i>	Down-regulates metastasis-related genes	[14, 33]
miR-200c	<i>BM11</i> , <i>ZEB1</i> , <i>ZEB2</i> , <i>TUBB3</i> , <i>FAP1</i>	Down-regulated in BC stem cells; prevents epithelial-mesenchymal transition; shows tumor suppressing properties in various experimental conditions; regulates apoptosis; higher expression level in well- vs. poorly-differentiated tumor cells	[34–36]
miR-18a	<i>ERalpha</i>	Regulates estrogen signaling; higher expression in ER-negative tumors	[37–39]
miR-205	<i>HER3</i> , <i>ZEB1</i> , <i>ZEB2</i> , <i>VEGF-A</i>	Down-regulated in BC; inhibits epithelial-mesenchymal transition	[40–42]
Dual role (?): evidence for both oncogenic and tumor suppressor activity			
miR-17-5p (miR-91)	<i>AIB1</i> , <i>CCND1</i> , <i>E2F</i> , <i>HBPI</i>	Regulates cell proliferation, invasion and migration	[14, 43, 44]

Table 2 Clinical characteristics of bilateral and unilateral tumors included in the study

Clinical characteristics	biBC							Total (n = 80)	uBC (n = 40)
	Paired biBC samples				Non-paired biBC samples				
	Synchronous (16 patients)		Metachronous (11 patients)		Synchronous (n = 14)	First tumor (n = 6)	Second tumor (n = 6)		
	Left (n = 16)	Right (n = 16)	First tumor (n = 11)	Second tumor (n = 11)					
Mean age at diagnosis	57.3		53.1	63.1	56.9	60.2	59.8	57.8	56.8
Age range	38–74		37–77	49–80	40–71	33–85	38–73	33–85	36–76
<i>T</i> status									
<i>T</i> = 1	8 (50%)	5 (31%)	4 (36%)	7 (64%)	6 (43%)	2 (33%)	4 (67%)	36 (45%)	14 (35%)
<i>T</i> > 1	8 (50%)	11 (69%)	7 (64%)	4 (36%)	8 (57%)	4 (67%)	2 (33%)	44 (55%)	26 (65%)
Concordance of <i>T</i> status within biBC pairs	11 (69%)		4 (36%)		–	–	–	–	–
<i>N</i> status									
<i>N</i> = 0	10 (67%)	10 (63%)	4 (36%)	9 (90%)	6 (46%)	5 (83%)	6 (100%)	50 (63%)	14 (35%)
<i>N</i> ≥ 1	5 (33%)	6 (38%)	7 (64%)	1 (10%)	7 (54%)	1 (17%)	0 (0%)	27 (34%)	26 (65%)
No data	1	–	–	1	1	–	–	3	–
Concordance of <i>N</i> status within biBC pairs	11 (69%)		2 (18%)		–	–	–	–	–
Menopausal status at the time of diagnosis									
Premenopausal	6 (38%)		4 (36%)	0 (0%)	4 (29%)	2 (33%)	1 (17%)	23 (30%)	13 (33%)
Postmenopausal	10 (63%)		7 (64%)	11 (100%)	10 (71%)	4 (67%)	5 (83%)	54 (70%)	27 (68%)
Family history									
Positive	1 (11%)		3 (30%)		4 (50%)	–	1 (17%)	13 (30%)	4 (10%)
Negative	8 (89%)		7 (70%)		4 (50%)	4 (100%)	5 (83%)	43 (70%)	36 (90%)
No data	7		1		6	2	–	24	–
Tumor histology									
Ductal	14 (88%)	14 (88%)	10 (91%)	11 (100%)	14 (100%)	6 (100%)	5 (83%)	74 (93%)	36 (90%)
Lobular	1 (6%)	2 (13%)	1 (9%)	–	–	–	1 (17%)	5 (6%)	1 (3%)
Mucinous	1 (6%)	–	–	–	–	–	–	1 (1%)	3 (8%)
ER status									
Positive	13 (81%)	12 (75%)	7 (64%)	6 (55%)	10 (71%)	3 (50%)	5 (83%)	56 (70%)	20 (69%)
Negative	3 (19%)	4 (25%)	4 (36%)	5 (45%)	4 (29%)	3 (50%)	1 (17%)	24 (30%)	9 (31%)
No data	–	–	–	–	–	–	–	–	11
Concordance of ER status within biBC pairs	15 (94%)		8 (73%)		–	–	–	–	–
PR status									
Positive	12 (75%)	11 (69%)	7 (64%)	5 (45%)	10 (71%)	3 (50%)	5 (83%)	53 (66%)	16 (55%)
Negative	4 (25%)	5 (31%)	4 (36%)	6 (55%)	4 (29%)	3 (50%)	1 (17%)	27 (34%)	13 (45%)

Table 2 continued
Clinical characteristics

	biBC				Non-paired biBC samples				Total (n = 80)	uBC (n = 40)
	Paired biBC samples		Metachronous (11 patients)		Synchronous (n = 14)	First tumor (n = 6)	Second tumor (n = 6)	Total (n = 80)		
	Synchronous (16 patients)	Left (n = 16)	Right (n = 16)	First tumor (n = 11)						
No data	-	-	-	-	-	-	-	-	11	
Concordance of PR status within biBC pairs	13 (81%)	-	5 (45%)	-	-	-	-	-	-	
HER2 status										
Positive	3 (19%)	1 (6%)	1 (9%)	0 (0%)	1 (7%)	1 (17%)	1 (17%)	8 (10%)	5 (22%)	
Negative	13 (81%)	15 (94%)	10 (91%)	11 (100%)	13 (93%)	5 (83%)	5 (83%)	72 (90%)	18 (78%)	
No data	-	-	-	-	-	-	-	-	17	
Concordance of HER2 status within biBC pairs	14 (88%)	-	10 (91%)	-	-	-	-	-	-	

Standard curves consisting of three tenfold dilutions of cDNA template were constructed for each analyzed miR. miR expression was scored as the ratio between relative quantity of target miR and relative quantity of miR-normalizer (miR-103). Uniform levels of expression of miR-103 in normal and cancerous tissues have been shown previously [47] and confirmed in the current study using the GeNorm algorithm [<http://medgen.ugent.be/~jvdesomp/genorm/>].

Statistical comparisons were made using SPSS 10 software package.

Results

The results of the miRs expression measurements are presented in Table 4 and Fig. 1. Strikingly, three miR species, i.e., miR-21, miR-10b, and miR-31, demonstrated higher level of expression in biBC as compared to uBC (Mann–Whitney $P = 0.0001, 0.00004, \text{ and } 0.0002$, respectively). Increased contents of miR-21, miR-10b, and miR-31 were observed in all categories of biBC tumors, i.e., in synchronous biBC as well as in first and second tumors from metachronous biBC pairs (Fig. 1). miR-155 and miR-18a showed significantly higher expression in estrogen ER-negative vs. ER-positive tumors (Table 4). miR-18a expression also demonstrated significant association with younger patients’ age; however, this relationship was purely attributed to the increased proportion of ER-negative tumors in women ≤ 50 years old (data not shown).

We also attempted to evaluate the level of similarity of miR expression status within tumor pairs (Fig. 2). We considered the ratio between miR expression scores within each pair as the measure of the level of concordance. All the tested miRs showed higher similarity of expression status in synchronous vs. metachronous biBC, that is statistically different from random distribution (binominal test $P \text{ value} = 0.004$). However, none of the individual miRs achieved the threshold for statistical significance (Fig. 2).

Discussion

This is the first study describing microRNA expression in bilateral breast carcinomas. Unexpectedly, two oncogenic miRs (miR-21, miR-10b) and one antioncogenic miR (miR-31) showed higher expression levels in tumors obtained from biBC patients as compared to unilateral neoplasms. Despite the relatively small sample size, this observation appears to have sufficient level of reliability. First, P values are indeed convincing, especially given the fact that they remained well below the significance threshold even after the adjustment for multiple comparisons

Table 3 Primers and probes for reverse transcription and real-time PCR

miR-21	
RT	GTCGTATCCAGTGCAGGGTCCGAGGTATTTCGCACTGGATACGACTCAACA
Forward	GCCGCTAGCTTATCAGACT
Probe	CGCACTGGATACGACTCAACAT
miR-10b	
RT	GTCGTATCCAGTGCAGGGTCCGAGGTATTTCGCACTGGATACGACCACAAAT
Forward	GCCGCTACCCTGTAGAAC
Probe	CGCACTGGATACGACCACAAAT
miR-17-5p	
RT	GTCGTATCCAGTGCAGGGTCCGAGGTATTTCGCACTGGATACGACCTACCT
Forward	GCCGCCAAAGTGCTTACAG
Probe	CGCACTGGATACGACCTACCT
miR-31	
RT	GTCGTATCCAGTGCAGGGTCCGAGGTATTTCGCACTGGATACGACAGCTATGC
Forward	GCCGCAGGCAAGATGCTG
Probe	TCGCACTGGATACGACAGCTATGC
miR-155	
RT	GTCGTATCCAGTGCAGGGTCCGAGGTATTTCGCACTGGATACGACACCCCTAT
Forward	GCCGCTTAATGCTAATCGTG
Probe	TCGCACTGGATACGACACCCCTA
miR-200c	
RT	GTCGTATCCAGTGCAGGGTCCGAGGTATTTCGCACTGGATACGACTCCATCAT
Forward	GCCGCTAATACTGCCGGGT
Probe	TCGCACTGGATACGACTCCATCA
miR-18a	
RT	GTCGTATCCAGTGCAGGGTCCGAGGTATTTCGCACTGGATACGACCTATCTGC
Forward	GCCGCTAAGGTGCATCTAGT
Probe	TCGCACTGGATACGACCTATCTGC
miR-205	
RT	GTCGTATCCAGTGCAGGGTCCGAGGTATTTCGCACTGGATACGACCAGACTC
Forward	GCCGCTCCTTCATTCCAC
Probe	TCGCACTGGATACGACCAGACT
miR-27a	
RT	GTCGTATCCAGTGCAGGGTCCGAGGTATTTCGCACTGGATACGACGCGGAAC
Forward	GCCGCTTCACAGTGGCTA
Probe	CGCACTGGATACGACGCGGAAC
miR-103	
RT	GTCGTATCCAGTGCAGGGTCCGAGGTATTTCGCACTGGATACGACTCATAGCC
Forward	CCGCAGCAGCATTGTACAG
Probe	CGCACTGGATACGACTCATAGC
Universal reverse primer	GTGCAGGGTCCGAGGTAT

(Table 4). Second, the observed trend was consistent in all the categories of biBC tumors (Fig. 2). Furthermore, the present study has confirmed a known bioclinical association, i.e., an increased expression of miR-155 and miR-18a in ER-negative breast carcinomas [26, 37, 38]; this implies that our sample set and methods of RNA analysis are comparable with the previously published studies.

The reasons of the differences in microRNA expression pattern between biBC and uBC are difficult to explain. It is

anticipated, that double occurrence of BC is characteristic for those women, who have particularly elevated genetic or non-genetic predisposition to breast cancer. Perhaps, development of BC in these highly predisposed subjects involves somewhat distinct repertoire of molecular events. Unfortunately, only a few prior investigations reported a direct comparison of somatic events in bilateral vs. unilateral breast carcinomas [9, 11, 12]. Sequencing of TP53 gene detected similar frequency of mutations in biBC and

Table 4 Median miR expression values in distinct BC subgroups

	biBC/uBC		Age		ER		Family history	
	biBC (<i>n</i> = 80)	uBC (<i>n</i> = 40)	≤50 (<i>n</i> = 38)	>50 (<i>n</i> = 82)	Negative (<i>n</i> = 76)	Positive (<i>n</i> = 33)	No (<i>n</i> = 79)	Yes (<i>n</i> = 17)
miR-21	1.01 (0.10–25.93)	0.56 (0.16–2.56)	0.79 (0.22–4.81)	0.80 (0.10–25.93)	0.91 (0.22–4.99)	0.84 (0.10–25.93)	0.77 (0.16–25.93)	0.92 (0.17–3.62)
<i>P</i>	0.0001*		0.55		0.42		0.97	
miR-10b	0.98 (0.01–18.52)	0.34 (0.02–2.70)	0.96 (0.02–5.26)	0.61 (0.01–18.52)	0.52 (0.01–4.37)	0.92 (0.03–18.52)	0.61 (0.02–18.52)	0.81 (0.03–7.75)
<i>P</i>	0.00004*		0.33		0.02		0.56	
miR-17-5p	0.76 (0.17–12.35)	1.22 (0.09–14.24)	0.97 (0.13–6.61)	0.68 (0.09–14.24)	0.95 (0.13–6.33)	0.72 (0.17–12.35)	0.93 (0.09–14.24)	0.50 (0.13–2.00)
<i>P</i>	0.05		0.09		0.19		0.002	
miR-31	0.94 (0.005–18.52)	0.40 (0.02–5.06)	1.11 (0.01–11.67)	0.63 (0.02–16.05)	1.16 (0.02–14.80)	0.65 (0.01–16.05)	0.67 (0.02–16.05)	1.21 (0.005–14.80)
<i>P</i>	0.0002*		0.03		0.04		0.40	
miR-155	0.65 (0.43–6.82)	0.85 (0.07–4.78)	0.86 (0.04–6.82)	0.67 (0.05–4.78)	1.24 (0.38–6.82)	0.63 (0.04–3.91)	0.83 (0.04–6.82)	0.63 (0.07–3.84)
<i>P</i>	0.04		0.02		0.00002*		0.31	
miR-200c	0.51 (0.12–6.38)	0.74 (0.16–4.73)	0.75 (0.14–2.92)	0.55 (0.12–6.38)	0.70 (0.33–2.92)	0.54 (0.12–6.38)	0.64 (0.15–6.38)	0.53 (0.12–1.62)
<i>P</i>	0.02		0.01		0.10		0.21	
miR-18a	0.45 (0.04–8.10)	0.32 (0.08–2.33)	0.50 (0.05–8.06)	0.35 (0.04–3.94)	0.96 (0.08–8.06)	0.36 (0.04–3.94)	0.39 (0.05–8.06)	0.44 (0.04–2.07)
<i>P</i>	0.01		0.0006*		0.000003*		0.86	
miR-205	0.38 (0.005–18.52)	0.40 (0.002–4.26)	0.55 (0.005–4.80)	0.33 (0.002–18.52)	0.38 (0.005–1.20)	0.38 (0.003–18.52)	0.38 (0.002–18.52)	0.46 (0.03–4.80)
<i>P</i>	0.57		0.005		0.22		0.29	
miR-27a	1.10 (0.16–13.58)	1.21 (0.07–26.97)	1.29 (0.35–4.35)	1.02 (0.07–26.97)	1.00 (0.35–26.97)	1.14 (0.07–13.58)	1.21 (0.07–27.00)	1.11 (0.30–3.88)
<i>P</i>	0.65		0.10		0.64		0.87	

Table 4 continued

	BRCA1		HER2		N status	
	Wild-type (n = 82)	Mutated (n = 7)	Negative (n = 94)	Positive (n = 14)	N = 0 (n = 64)	N > 0 (n = 53)
miR-21	0.72 (0.16–25.93)	1.21 (0.27–1.92)	0.84 (0.10–25.93)	0.78 (0.30–2.56)	0.74 (0.10–25.92)	0.83 (0.16–8.92)
<i>P</i>	0.27		0.93		0.73	
miR-10b	0.79 (0.02–18.52)	0.73 (0.16–4.00)	0.79 (0.01–18.52)	0.44 (0.18–4.37)	0.80 (0.01–18.52)	0.52 (0.03–7.75)
<i>P</i>	0.75		0.60		0.22	
miR-17- 5p	0.77 (0.09–14.24)	0.95 (0.29–1.65)	0.78 (0.13–12.35)	0.67 (0.36–4.04)	0.71 (0.09–12.34)	0.78 (0.13–14.24)
<i>P</i>	0.93		0.56		0.21	
miR-31	0.69 (0.01–16.05)	1.89 (0.22–5.35)	0.68 (0.01–16.05)	0.92 (0.09–7.93)	0.63 (0.02–16.05)	0.69 (0.005–14.80)
<i>P</i>	0.07		0.74		0.35	
miR-155	0.80 (0.04–6.82)	0.76 (0.32–2.74)	0.71 (0.04–6.82)	0.84 (0.38–4.78)	0.71 (0.05–5.00)	0.80 (0.04–6.82)
<i>P</i>	0.81		0.07		0.35	
miR-200c	0.65 (0.12–6.38)	0.47 (0.39–0.84)	0.55 (0.12–6.38)	0.74 (0.33–1.90)	0.55 (0.15–6.38)	0.60 (0.12–2.92)
<i>P</i>	0.25		0.24		0.64	
miR-18a	0.37 (0.04–8.06)	0.50 (0.10–4.21)	0.41 (0.04–8.06)	0.55 (0.08–1.57)	0.40 (0.04–8.06)	0.39 (0.05–2.75)
<i>P</i>	0.20		0.41		0.91	
miR-205	0.41 (0.002–18.52)	0.24 (0.07–2.50)	0.38 (0.005–18.52)	0.43 (0.003–1.77)	0.34 (0.002–18.52)	0.42 (0.003–4.80)
<i>P</i>	0.31		0.78		0.18	
miR-27a	1.23 (0.07–13.58)	0.71 (0.26–1.63)	1.11 (0.07–13.58)	1.09 (0.59–26.97)	1.00 (0.16–13.58)	1.33 (0.07–27.00)
<i>P</i>	0.14		0.69		0.03	

Minimal and maximal expression values are given in parentheses. Comparisons were performed using Mann–Whitney *U* test. *P* values, which remained below 0.01 after Holm’s adjustment for multiple comparisons [48], are designated by asterisks. BRCA1 status assessment was done in all patients irrespectively of their age or family history; it included testing for three founder mutations (5382insC, 4153delA, and 185delAG), which constitute over 90% BRCA1 defects in Russia [49, 50]

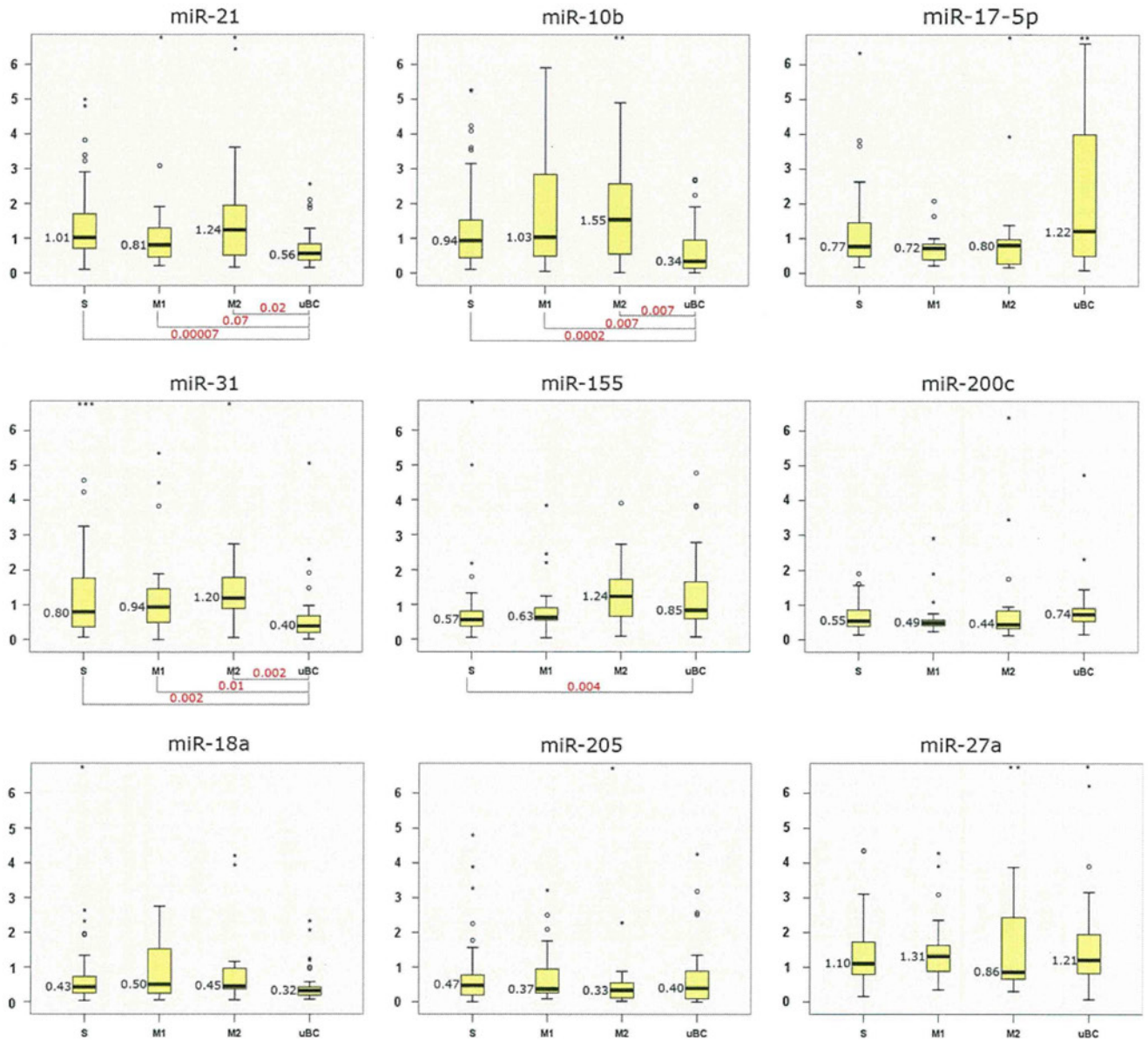


Fig. 1 MicroRNA expressions in biBC and uBC. *S* tumors from synchronous biBC; *M1* and *M2* First and second tumors from metachronous biBC. *Central bars* indicate median expression values, boxes correspond to the first and third quartiles of the variations, *lower and upper bars* show the non-outlier range. Outliers are the

samples located in more than 1.5 interquartile range (IQR) outside the corresponding box. *Circles and asterisks* designate minor (1.5–3 IQR) and major (>3 IQR) outliers, respectively. Significant *P* values are given below the plots

uBC; however, tumors from synchronous biBC pairs tended to contain multiple nucleotide alterations within this gene, that was interpreted as potential indicator of genotoxic stress or failed genome defense [12]. A subset of contralateral neoplasms from metachronous biBC, but not other categories of breast tumors, were shown to have the so-called microsatellite instability phenotype (MSI-H); this observation was linked to the mutagenic effect of the adjuvant therapy applied for the treatment of the first malignancy [11]. Furthermore, first tumors from the

metachronous biBC pairs demonstrated lower frequency of oncogene amplifications than second cancers from the same patients, synchronous biBC or unilateral BC; this difference was explained by the adverse prognostic role of oncogene extra copies, i.e., by reduced chances of amplification-positive BC patients to survive until the development of new malignancy [9]. While TP53 mutations, MSI-H status, and gene amplifications showed non-random distribution only within specific categories of biBC tumors, elevated levels of miR-21, miR-10b, and miR-31

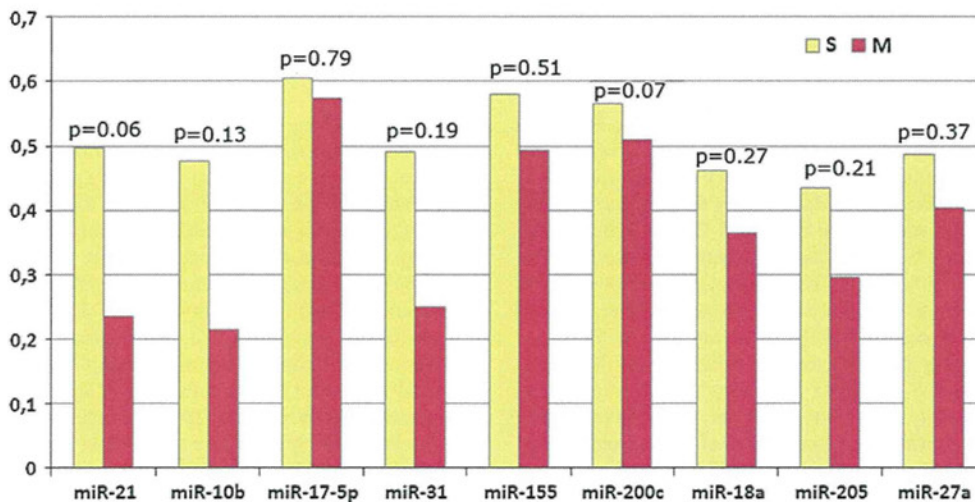


Fig. 2 Concordance of microRNA status in synchronous vs. metachronous biBC. Ratio between higher and lower expression score within a given biBC pair was considered as the measure of the similarity of miR status. Columns represent the inverse median value of this ratio, so higher columns correspond to higher level of concordance. All the

expressions were documented across all biBC subsets (Fig. 1). This observation suggests that the expression-modulating event is relatively stable over time, therefore it is more likely to be genetic than environmental. For example, BRCA-related breast cancers are well known to have specific molecular portraits [51]; however, BRCA1 mutation status did not influence miR expression in the present study (Table 4). It is possible that the other, yet unknown genetic features of the host contribute to the distinct patterns of miR-21, miR-10b, and miR-31 expression in biBC.

This investigation has demonstrated higher similarity of tumor characteristics in synchronous vs. metachronous biBC doublets both for essential clinical features and for microRNA expression profiles (Table 2, Fig. 2). This trend is consistent with the previous studies involving paired biBC samples [5–8]. One of the explanations of phenotypic concordance of the tumors within biBC pairs includes possible metastatic nature of a subset of contralateral BC. However, virtually all available evidence suggest that a misdiagnosis between true double primary and BC metastasis to the opposite breast is exceptionally rare [1, 5, 9]. Given that synchronous biBC arise in nearly identical circumstances, i.e., age of the patient, hormonal or metabolic milieu, and history of exposure to various hazards, it is logical to expect that these tumor pairs are likely to share central events of tumor pathogenesis, including changes in the microRNA expression levels.

In conclusion, this study has shown distinct patterns of microRNA expression in bilateral vs. unilateral breast carcinomas and revealed a trend toward concordance of miR profiles within synchronous biBC pairs.

studied miRs showed more similarity of expression status in synchronous vs. metachronous biBC ($P = 0.004$ by the binominal test). However, none of the individual miRs achieved significant Mann–Whitney P value

Acknowledgments This study has been supported by the Russian Federation for Basic Research (grants 10-04-92110, 10-04-00260, 11-04-00227 and 11-04-01643), the Japanese Society for the Promotion of Science (JSPS) (project 10037711), the Federal Agency for Science and Innovations (contract 02.740.11.0780), the Commission of the European Communities (grant PITN-GA-2009-238132), and the Government of Moscow (grant 15/11).

Conflict of interest None.

References

1. Imyanitov EN, Hanson KP (2003) Molecular pathogenesis of bilateral breast cancer. *Cancer Lett* 191:1–7
2. Kuligina E, Reiner A, Imyanitov EN, Begg CB (2010) Evaluating cancer epidemiologic risk factors using multiple primary malignancies. *Epidemiology* 21:366–372
3. Chen Y, Thompson W, Semenciw R, Mao Y (1999) Epidemiology of contralateral breast cancer. *Cancer Epidemiol Biomarkers Prev* 8:855–861
4. Majed B, Dozol A, Ribassin-Majed L, Senouci K, Asselain B (2011) Increased risk of contralateral breast cancers among overweight and obese women: a time-dependent association. *Breast Cancer Res Treat* 126:729–738
5. Imyanitov EN, Suspitsin EN, Grigoriev MY, Togo AV, ESh Kuligina, Belogubova EV, Pozhariski KM, Turkevich EA, Rodriguez C, Cornelisse CJ, Hanson KP, Theillet C (2002) Concordance of allelic imbalance profiles in synchronous and metachronous bilateral breast carcinomas. *Int J Cancer* 100: 557–564
6. Park SC, Hwang UK, Ahn SH, Gong GY, Yoon HS (2007) Genetic changes in bilateral breast cancer by comparative genomic hybridisation. *Clin Exp Med* 7:1–5
7. Huo D, Melkonian S, Rathouz PJ, Khramtsov A, Olopade OI (2011) Concordance in histological and biological parameters between first and second primary breast cancers. *Cancer* 117: 907–915